A Simple Way to Fabricate Close-Packed High Numerical Aperture Microlens Arrays

Xiangwei Meng, Feng Chen, Qing Yang, Hao Bian, Hewei Liu, Pubo Qu, Yang Hu, Jinhai Si, and Xun Hou

***Abstract*— We present a developed femtosecond laser enhanced wet chemical etching method to fabricate close-packed and high numerical aperture (NA) microlens arrays (MLAs). Its ability to fabricate 100% fill factor MLAs with controllable NA is demonstrated and the maximum NA value of the lenses reaches to 0.47. This letter provides a simple and efficient way to achieve controllable and low cost optical elements. The close-packed and high-NA properties lead to excellent optical performance of the MLAs, which are highly required in high-resolution and high-signal-to-noise-ratio detections in micro-optical and integrated optical applications.**

***Index Terms*— Femtosecond laser, high numerical aperture, microlens array, silica glass.**

I. Introduction

MICROLENSES and microlens arrays (MLAs) with diameters of a few to hundreds micrometers are widely used in micro-manufacturing, display and image sensing due to the enhancement light collimation and collection efficiency [1]–[4]. Fill factor and numerical aperture (NA) are two critical parameters that influence the optical performance of the MLAs. High-fill-factor MLAs will capture most incident lights to increase the signal-noise-ratio, and high-NA microlenses can generate high-resolution images. These characteristics are highly required in optical interconnects, bio-detection system, laser protection goggle, 2D optical data recording and projection systems [4], [5]. Close-packed high numerical aperture microlens arrays are continuously pursued.

However, close-packed MLAs with high NA is still challenging for most current processing techniques. For example, thermal reflow methods [6], [7], ink-jet processes of UV curable polymers [8], hot embossing techniques [9] and laser direct writing [10] can produce MLAs with low and intermediate NA, typically 0.1∼0.3. For fabricating the high NA MLAs, self-assembly [11], UV-assisted curing of microfluidic networks [12], atop polymethylmethacrylate (PMMA) immersion in ethanol [13], [14] and glass microspheres trapped on microholes with a thin polymer layer method [15] were demonstrated, but the fill factor of these high NA MLAs were low. More importantly, it is difficult for most aforementioned methods to control the NA values of the microlenses.

Recently, femtosecond (fs) laser direct writing process was used to fabricate high fill factor and high NA (NA∼0.46) MLAs has also been performed [16], [17]. This method can produce microlenses with nanometer surface accuracies and controllable NA values, but the used materials were limited to a few types of photo-curable polymers which have lower light transmittances and mechanical strengths than other plastics, polymers and glasses. Additionally, because the laser direct writing process was time-consuming, the pixel number of the MLAs would not be high enough.

In the previous work of our group, a fs laser enhanced local wet etching method was proposed for fabricating high quality MLAs on silica glass [18], [19] and glass cylindrical [20], [21]. The focused fs laser triggers a series of complex material responses and change its physical and chemical propertied in the focal spots; the concave MLAs with smooth surfaces then are formed in those laser-modified spots with the aid of chemical wet etch. But the depth of modified regions are limited in the exposure process, the NA of MLAs obtained is lower than 0.26. Herein, we present a developed approach for high-efficiency fabrication of high NA concave MLAs on silica glasses. Combining laser vertical deep scanning exposures and wet etch process, microlens arrays are closed-packed with 100% fill factors, and the NA of the lenses can be controlled in a range from 0.17 to 0.47. We also demonstrate the ability to adjust the size and NA of MLAs by controlling the laser parameters, scanning depth and etch time. The fabricated concave structures can be used as molding templates for replicating low-cost polymer MLAs. The high-resolution imaging properties of the MLAs are also demonstrated.

II. Method and Experiment

The fabrication process of the high NA MLAs is presented in Fig. 1. The sample used in the experiment is polished silica glass ($20 \times 20 \times 2$ mm^3, China Daheng Group Inc., GCL-1202). A Ti: sapphire pulsed laser with 50 fs, 1 kHz and 800 nm is used in the experiment. There is a quarter wave plate used to change the linear polarization laser to circular polarization. The incident pulse energy can be varied by a variable neutral density filter and the laser power is adjusted to 5 mW. The laser beam is vertically focused by a 50× objective lens (NA = 0.50, Olympus). The diameter of the focal spot is about 1.4 μm (1/e). The exposure time is controlled by a

Manuscript received August 23, 2012; revised February 5, 2013; accepted May 7, 2013. Date of publication May 23, 2013; date of current version July 2, 2013. This work was supported in part by the National Science Foundation of China under Grant 61176113, in part by the National High Technology R&D Program of China under Grant 2009AA04Z305, and in part by the Fundamental Research Funds for the Central Universities.

The authors are with the State Key Laboratory for Manufacturing Systems Engineering and Shanxi Key Laboratory of Information Photonic Technique, Xi'an Jiaotong University, Xi'an 710049, China (e-mail: chenfeng@mail.xjtu.edu.cn).

Color versions of one or more of the figures in this letter are available online at http://ieeexplore.ieee.org.

Digital Object Identifier 10.1109/LPT.2013.2264801

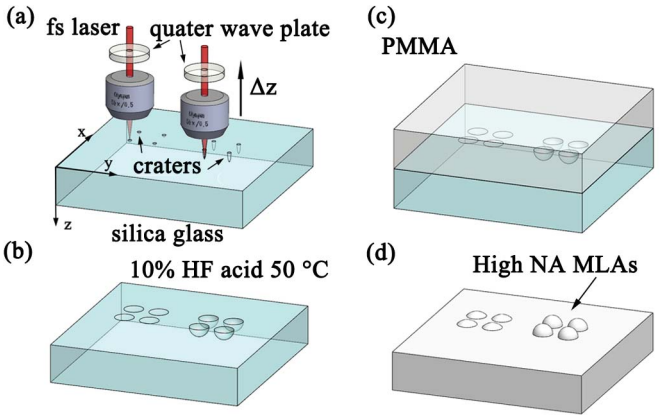

Fig. 1. Schematic diagrams of the fabrication procedures of the high NA MLAs (a) arrays of the laser vertical scanning exposures deep craters are ablated on a silica glass; (b) concave MLAs with spherical surface are formed by chemical wet etching process. (c) and (d) show the replication procedure of convex PDMS MLAs.

shutter. The sample is fixed onto a computer-controlled three dimensions stage.

In the laser exposure process, in order to get the deep crater, straight regions of modification were made by translating the sample parallel to the direction of the laser beam propagation, the z-axis, and the scanning depth, Δz is programmed control from 0 to 100 μm with a speed of 10 μm/s (Fig. 1(a)). After the laser exposures, the samples were immersed in 10% hydrofluoric acid (HF) solution at 50 °C (Fig. 1(b)). The warm environment can benefit to improve the etch rate. In this course, the etch rate of the laser irradiated regions is much more rapid than the non-irradiated regions. Then the laser irradiation regions begin to form the concave smooth surfaces and the MLAs are consequently fabrication in tens of minutes. The curvature radius of the etched surfaces increases with the scanning depth, Δz. So the MLAs mold with the varied NA on silica glasses are obtained in the etching results. After the chemical etching process, the samples are cleaned by the ultrasonic bath in acetone, alcohol and deionized water for 15 minutes, respectively. The fabrication process can be monitored by an optical microscope equipped with a CCD camera.

Then the concave structures on the silica glass could be used as a mold to replicate the convex MLAs on ploymers. To form the convex MLAs on the planar sheet, a dilute chloroform solution of PMMA with a mass concentration of 0.10 g/ml was dropped on MLAs mold. The PMMA solution rapidly spreads out evenly and solidifies to a thin film in a clean bench (Fig. 1(c)). The effect of the surface tension results in a good surface uniformity and the convex MLAs was then formed, which was easily stripped from the glass by the ultrasonic bath in deionized water (Fig. 1(d)). The thickness of the PMMA film was controlled by the concentration of the PMMA solution.

The morphologies of the concave MLAs mold on the silica glass and the convex MLAs on the PMMA were measured by a scanning electronic microscope (SEM, Hitachi S-3000N). The cross-sectional and 3D profiles of the microlens were measured by a laser scanning confocal microscope (LSCM, OLYMPUS OLS4000). The images capability of the MLAs was obtained by an optical microscope system (OM, NIKON CV-100) with a tungsten light source and a CCD camera.

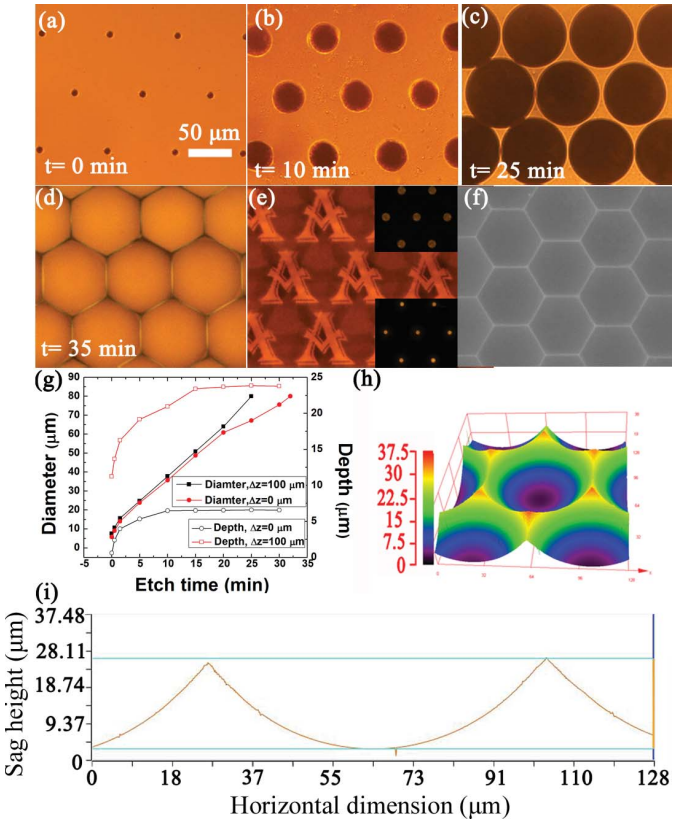

Fig. 2. The results of 100% fill factor MLAs with high NA on the silica glass. (a), (b), (c), and (d) The formation process of the concave microstructures during the chemical etching. The craters arrays on the silica glass irradiation by fs laser pulses with the scanning depth, $\Delta z = 100$ μm and an interspacing of 80 μm. (e) The images of the letter "A" and focal spots generated by the MLAs. (f) The SEM image of MLAs. (g) The evolution of the diameter and depth of structures versus the wet-etching time. (h) and (i) are the results of concave MLAs measured by LSCM.

III. Results and Discussion

To achieve high NA, microlens should have small curvature radius, thus the same diameter of lens with high NA requires a larger convex or concave height. In order to get the same diameters of MLAs with different sag heights, h, we fixed the distance of the adjacent craters at 80 μm. The deep craters on the silica glasses were ablated with the scanning depth, Δz, of 100 μm and the laser power of 5 mW, as shown in Fig. 2(a). The emission particles ablated by the fs laser stayed in the craters to block the laser, and the increasing spherical aberration produced by the glass surface at increased scanning depth presumably weakened the following laser against the following ablation. The diameter D and depth h of the craters were about 7.5 μm and11.25 μm, respectively.

When the glass was immersed in the 10% HF acid solution at about 50 °C, materials inside the crater were rapidly etched out. The irradiation regions were modified by a series of laser induced effects, which have higher etching velocity than the unexposed materials. The orientation of the laser-induced structures and modification tracks by linear polarization laser

were perpendicular to the scanning direction and had stop-layers hindering the etching progress, which were reported by Hnatovsky *et al*. [22], [23]. So we used the circle polarization laser to ablate the glass to disturb the orientation of the ablation results, which had the higher etch rates. In the first one minute, the values of D and h have reached to about 13.24 μm and 14.12 μm; the etching velocities in diameter and depth directions at this period were about 5 μm/min and 3 μm/min, respectively. The micro-craters were expanded and progressively formed circular patterns (Fig. 2(b)). The values then decreased in the following 5 minutes and declined to about 3 μm/min and 0.7 μm/min at about 20 minutes, respectively, as shown in Fig. 2(g). The following etching process was to smooth and expand the surface, and then the etching velocity of the concave surface was identical to that of unexposed materials. After 15 minutes, the diameter of the structures increased linearly and therefore the sag height was a constant. The diameter of the circular microlens expanded gradually, and eventually, the adjacent ones "overlapped" with each other resulting in formation of the hexagonal-shaped microlens (Fig. 2(b) and (c)). Then the gaps between the microlenses were disappeared and the fill factor of MLAs mold on silica glass was achieved 100% (Fig. 2(d)). In order to investigate optical properties of the high fill-factor MLAs mold on the silica glass, the images were captured by a microscopic objective lens and a CCD camera which were placed on the other side of the MLAs [19]. We used a mask with a transparent letter, "A", which was printed on a small piece of film about 20 × 20 mm^2. Fig. 2(e) shows the imaging ability of the concave MLAs mold on the silica glass. The inset images in Fig. 2(e) were the focal spots of the MLAs with the scanning depth of 0 μm (top) and 100 μm (bottom).

The SEM image of the fabricated hexagonal microstructures was shown in Fig. 2(f), demonstrating the ability to fabricate high-ordered uniform and smooth microlenses by this method. The 3D profiles and cross-section profiles were measured by the LSCM and the results were shown in Fig. 2(g) and (h). The measured values of radius and sag height of the concave microlens were 38.2 μm and 23.86 μm, respectively. The standard deviation of the radius and height were 1.7% and 1.4%, respectively. The measured diameter of 76.4 μm was close to the distance between the adjacent focal spots.

The optical parameters of the MLAs, including the radius of curvature, R, focal length, f, f-number, $f_{\#}$, and NA were estimated by the following equations:

$$R = \frac{h^2 + r^2}{2h} \tag{1}$$

$$f = \frac{R}{n-1} \tag{2}$$

$$f_{\#} = \frac{f}{2r} \tag{3}$$

$$NA = \frac{D}{2f} \tag{4}$$

where r and h were the radius and the sag height of a microlens, respectively, and n was the refractive index of the material ($n = 1.52$ for silica glass and $n = 1.49$ for PMMA at 589.3 nm). From the equations (1)∼(4), it was shown that

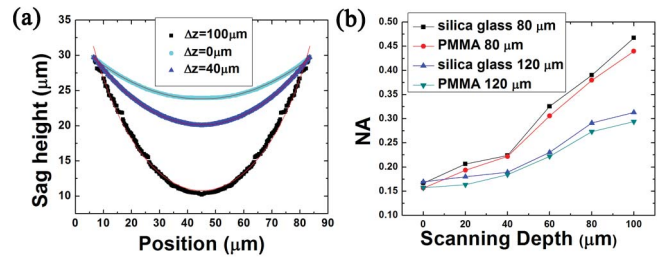

Fig. 3. (a) The cross-section of the MLAs with an interspacing of 80 μm are presentation with the scanning depth, $\Delta z = 0$ μm, 40 μm, and 100 μm. (b) The relationship between scanning depth and the NA of MLAs. The square symbol and circle symbol are presentation silica glass MLAs and PMMA MLAs, the triangle symbol and inverted triangle symbol are presentation silica glass MLAs and PMMA MLAs with the interspacing of 120 μm, respectively.

the optical parameters of the MLAs were determined together by the diameter, D, and the sag height, h. In our experiment, the diameter and sag height were controlled by the distance of the arrangement of the adjacent laser ablation craters and the scanning depth, Δz, respectively. The diameter and sag height of concave MLAs on silica glass with the distance of the adjacent ablation craters, 80 μm, and the scanning depth, $\Delta z = 100$ μm were 76.4 μm and 23.86 μm, respectively. The NA of ∼0.47 of the MLAs mold on the silica glass was obtained by equation (1)∼(4).

As mentioned above, the D and h were the critical parameter to NA. The diameters of microlenses were fixed by controlling the adjacent distances between focal spots. The depth of the microlens increased with the scanning depth, Δz (Fig. 3(a)) and the cross-section of the MLAs mold on the silica glass were well fitted by the semi-circle functions. So the microlens with deeper scanning depth had a higher NA. It could be seen from Fig. 3(b) that the NA of the MLAs mold followed a linear tendency with the scanning depth, Δz. The calculated NA of MLAs mold on the silica glass ranged from 0.17 to 0.47 with the focal spots distance of 80 μm and 0.17 to 0.31 with the focal spots distance of 120 μm, respectively (Fig. 3(b)).

The fabricated on silica glasses were subsequently used to replicate convex MLAs on PMMA. The radius and sag height of MLAs mold were 60.06 μm and 9.90 μm, respectively. The replication results were measured by the LCSM. The 3D and cross-section profiles of the MLAs were given in Figs. 4(a) and (b), respectively. The measured radius and sag height were 58.91 μm and 9.75 μm. Comparing the mold and the replication MLAs, the replication consistency of the diameters and sag-heights were about 98.1% and 98.5%, respectively, indicating that the PMMA MLAs were faithfully replicated. The PMMA was under-filled in silica mold, and when the PMMA become dry, it shrunk slightly. So the replication was slightly smaller than the original mold. The calculated NA of MLAs on PMMA ranged from 0.16 to 0.44 with the focal spots distance 80 μm and 0.16 to 0.30 with the focal spots distance 120 μm, respectively (Fig. 3(b)). Consequently, the image was observed and appeared the high quality imaging ability of the MLAs on the PMMA, as shown in Fig. 4(c).

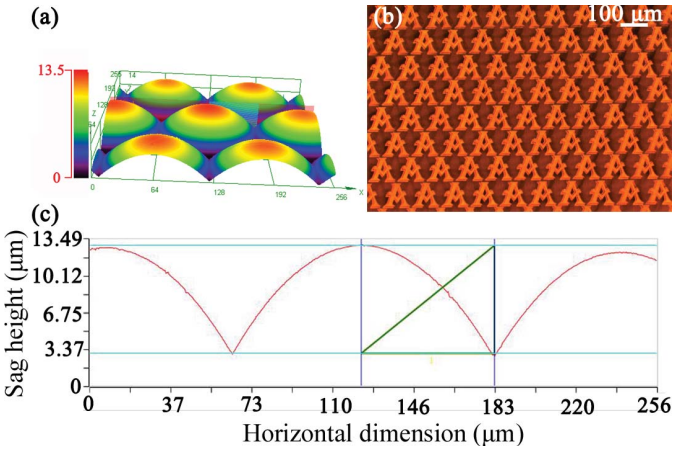

Fig. 4. The results of the replicated MLAs with an interspacing of 120 μm. (a) and (b) The images of the letter "A" generated by the replicated MLAs. (c) presents the 3D and cross-section profiles of the MLAs on PMMA.

IV. Conclusion

We have presented a novel method to fabricate concave MLAs with high NA and 100% fill-factor on the silica glasses. The high surface quality, high uniformity and high imaging performance of the MLAs are also demonstrated. By controlling the scanning depth of the craters, etch time and arrangement of the exposure spots, NA controllable MLAs with high imaging quality are achieved. The fabricated concave mold with hexagonal-shaped structures is also used to replicate convex MLAs on PMMA. Our approach offers several advantages, such as high imaging quality, high efficiency, low-cost, easy manipulation, and reproducible fabrication process. We should also note that the silica mold can also used in the hot embossing and UV-light curing process to fabricated MLAs on other polymers.

References

[1] M. H. Wu, C. Park, and G. M. Whitesides, "Fabrication of arrays of microlenses with controlled profiles using gray-scale microlens projection photolithography," *Langmuir*, vol. 18, no. 24, pp. 9312–9318, 2002.

[2] S.-I. Chang, J.-B. Yoon, H. Kim, J.-J. Kim, B.-K. Lee, and D. H. Shin, "Microlens array diffuser for a light-emitting diode backlight system," *Opt. Lett.*, vol. 31, no. 20, pp. 3016–3018, 2006.

[3] A. Deutsch, *et al.*, "Microplate cell-retaining methodology for high-content analysis of individual non-adherent unanchored cells in a population," *Biomed. Microdevices*, vol. 8, no. 4, pp. 361–374, 2006.

[4] J. N. Kuo, C. C. Hsieh, S. Y. Yang, and G. B. Lee, "An SU-8 microlens array fabricated by soft replica molding for cell counting applications," *J. Micromech. Microeng.*, vol. 17, no. 4, p. 693, 2007.

[5] K. H. Jeong and L. P. Lee, "A new method of increasing numerical aperture of microlens for biophotonic MEMS," in *Proc. 2nd Annu. Int. IEEE-EMB Special Topic Conf. Microtechnol. Med. Biol.*, May 2002, pp. 380–383.

[6] C. P. Lin, H. Yang, and C. K. Chao, "Hexagonal microlens array modeling and fabrication using a thermal reflow process," *J. Micromech. Microeng.*, vol. 13, no. 5, pp. 775–781, 2003.

[7] E. Roy, B. Voisin, J. F. Gravel, R. Peytavi, D. Boudreau, and T. Veres, "Microlens array fabrication by enhanced thermal reflow process: Towards efficient collection of fluorescence light from microarrays," *Microelectron. Eng.*, vol. 86, no. 11, pp. 2255–2261, 2009.

[8] S. Biehl, R. Danzebrink, P. Oliveira, and M. A. Aegerter, "Refractive microlens fabrication by ink-jet process," *J. Sol-Gel Sci. Technol.*, vol. 13, nos. 1–3, pp. 177–182, 1998.

[9] N. Ong, Y. Koh, and Y. Q. Fu, "Microlens array produced using hot embossing process," *Microelectron. Eng.*, vol. 60, nos. 3–4, pp. 365–379, 2002.

[10] T. Chen, T. Wang, Z. Wang, T. Zuo, J. Wu, and S. Liu, "Microlens fabrication using an excimer laser and the diaphragm method," *Opt. Express*, vol. 17, no. 12, pp. 9733–9747, 2009.

[11] J.-Y. Huang, Y.-S. Lu, and J. A. Yeh, "Self-assembled high NA microlens arrays using global dielectricphoretic energy wells," *Opt. Express*, vol. 14, no. 22, pp. 10779–10784, 2006.

[12] A. Tripathi, T. V. Chokshi, and N. Chronis, "A high numerical aperture, polymer-based, planar microlens array," *Opt. Express*, vol. 17, no. 22, pp. 19908–19918, 2009.

[13] Y. Zhao, C. C. Wang, W. M. Huang, H. Purnawali, and L. An, "Formation of micro protrusive lens arrays atop poly(methyl methacrylate)," *Opt. Express*, vol. 19, no. 27, pp. 26000–26005, 2011.

[14] Y. Zhao, W. M. Huang, and H. Purnawali, "Three dimensional surface patterning atop poly(methyl methacrylate)(PMMA)," *Appl. Mech. Mater.*, vol. 161, pp. 292–295, Mar. 2012.

[15] A. Tripathi and N. Chronis, "A doublet microlens array for imaging micron-sized objects," *J. Micromech. Microeng.*, vol. 21, no. 10, p. 105024, 2011.

[16] W. Dong, *et al.*, "Femtosecond laser rapid prototyping of nanoshells and suspending components towards microfluidic devices," *Lab Chip*, vol. 9, pp. 2391–2394, Aug. 2009.

[17] D. Wu, *et al.*, "High numerical aperture microlens arrays of close packing," *Appl. Phys. Lett.*, vol. 97, no. 3, p. 031109, 2010.

[18] F. Chen, *et al.*, "Maskless fabrication of concave microlens arrays on silica glasses by a femtosecond-laser-enhanced local wet etching method," *Opt. Express*, vol. 18, pp. 20334–20343, Sep. 2010.

[19] B. Hao, *et al.*, "Versatile route to gapless microlens arrays using laser-tunable wet-etched curved surfaces," *Opt. Express*, vol. 20, no. 12, pp. 12939–12948, 2012.

[20] Z. F. Deng, *et al.*, "A facile method to fabricate close-packed concave microlens array on cylindrical glass," *J. Micromech. Microeng.*, vol. 22, p. 115026, Nov. 2012.

[21] G. Q. Du, *et al.*, "Direct fabrication of seamless roller molds with gapless and shaped-controlled concave microlens arrays," *Opt. Lett.*, vol. 37, pp. 4404–4406, Nov 2012.

[22] C. Hnatovsky, R. S. Taylor, E. Simova, V. R. Bhardwaj, D. M. Rayner, and P. B. Corkum, "Polarization-selective etching in femtosecond laser-assisted microfluidic channel fabrication in fused silica," *Opt. Lett.*, vol. 30, no. 14, pp. 1867–1869, 2005.

[23] S. Ho, P. R. Herman, and J. S. Aitchison, "Single-and multi-scan femtosecond laser writing for selective chemical etching of cross section patternable glass micro-channels," *Appl. Phys. A, Mater. Sci. Process.*, vol. 106, no. 1, pp. 5–13, 2012.